ADVANCED MATERIALS TECHNOLOGIES

www.advmattechnol.de

A Highly Sensitive Capacitive-Based Soft Pressure Sensor Based on a Conductive Fabric and a Microporous Dielectric Layer

*Ozgur Atalay, Asli Atalay, Joshua Gafford, and Conor Walsh**

In this paper, the design and manufacturing of a highly sensitive capacitive-based soft pressure sensor for wearable electronics applications are presented. Toward this aim, two types of soft conductive fabrics (knitted and woven), as well as two types of sacrificial particles (sugar granules and salt crystals) to create micropores within the dielectric layer of the capacitive sensor are evaluated, and the combined effects on the sensor's overall performance are assessed. It is found that a combination of the conductive knit electrode and higher dielectric porosity (generated using the larger sugar granules) yields higher sensitivity (121×10^{-4} kPa^{-1}) due to greater compressibility and the formation of air gaps between silicone elastomer and conductive knit electrode among the other design considerations in this study. As a practical demonstration, the capacitive sensor is embedded into a textile glove for grasp motion monitoring during activities of daily living.

The development of flexible and soft pressure sensors is gaining attention due to applications in wearable electronic devices,[1–9] soft robotics,[10–16] and human–machine interactive systems.[17–20] Applications of daily use for wearable systems (such as tactile perception and object manipulation) require pressures that range from 1 to 100 kPa pressure.[21] Thus, to have sufficient sensory coverage over the anticipated tactile pressure range, it is essential to have highly sensitive sensors capable of measuring pressures in excess of 100 kPa. In order to fulfill this aim, various types of sensing technologies have been explored that utilize capacitive,[22–26] piezoresistive,[27–31] or piezoelectric[32,33] sensing modalities. Among these approaches, parallel plate capacitive sensing technology is popular due to signal repeatability, temperature insensitivity, and relative simplicity of design and construction.[34,35] In this approach, when an external force is applied to the soft pressure sensor, the dielectric layer thickness of the sensor varies, which leads to a change in the capacitance of the sensor. However, due to relatively small changes in the capacitance of parallel plate sensors under loading, achievable sensitivities are typically very low.[21] Therefore, most studies focus on the modification of the dielectric layer to increase sensitivity. In this context, efforts toward increased sensitivity can be grouped into two main categories: surface modification of the elastomer layers and the creation of micropores within the dielectric layer. In the first approach, topographical features[36–40] (such as nanoscale pyramids, microstructured line patterns, or micrometer-scale circular pillars) are created on the elastomer surface via surface micromachining methods (such as photolithography and molding). However, It should be noted here that, even though high sensitivity can be achieved using surface micromachining, the working range is typically limited to <10 kPa that is undesirable for most wearable applications. The latter approach focuses on the creation of a porous dielectric layer[41–44] and a recent trend is to use solid particle leaching[44–48] to create micropores within the silicone elastomer. As commercially available sugar cubes and silicone elastomers can be used, manufacturing is quick, simple, and low cost. It has been shown that increased sensitivity over the tactile pressure range was achieved using this method due to the reduced stiffness of the dielectric material as well as increased effective dielectric constant due to the presence of air gaps within the microporous structure. Capacitance values are typically on the order of several femtofarads due to the dielectric layer thickness (height of the sugar cube templates is around 10 mm), but a higher baseline capacitance is needed for sufficient signal-to-noise in the presence of parasitic capacitances within the readout circuitry in these systems. Beside, carbon-based materials,[46] conductive thin films[48] are generally employed to construct electrode layers and are used in combination with the modified dielectric layer for the formation of the soft sensor. However, to integrate these sensors into the system for the creation of wearable electronic devices, the sensors themselves must be flexible, robust, and have mechanically

Dr. O. Atalay
Faculty of Textile Technologies and Design
Istanbul Technical University
Istanbul 34437, Turkey
Dr. A. Atalay
Faculty of Technology, Textile Engineering Department
Marmara University
Istanbul Turkey
J. Gafford, Prof. C. Walsh
Harvard John A. Paulson School of Engineering and Applied Sciences
Harvard University
Cambridge, MA 02138, USA
E-mail: walsh@seas.harvard.edu
Dr. O. Atalay, Dr. A. Atalay, J. Gafford, Prof. C. Walsh
Wyss Institute for Biologically Inspired Engineering
Harvard University
Boston, MA 02115, USA

DOI: 10.1002/admt.201700237

secure electrical connections within the sensor body. In addition, the sensor must have a robust conductive network within the electrode layer that retains its properties over the anticipated loading range. Finally, the sensors must be easily integrated into the wearable system without deterioration of the sensor's intrinsic properties. Thus, we took into account above considerations for the proposed sensor design. Given these requirements, conductive textile structures are good candidates to meet the aforementioned challenges, as shown in some previous works.

In this work, we demonstrate fast and easy fabrication of a flexible capacitive pressure sensor made with conductive fabric electrodes and a microstructured silicone dielectric layer for wearable electronic applications. We achieved the thin dielectric layer (less than 1 mm thick) by mixing solid sacrificial particles with silicone elastomer and pouring the mixture into 3D printed molds. The thin dielectric layer leads to a higher baseline capacitance, thereby making the sensors more robust to parasitic capacitance in the readout circuitry and increasing the signal-to-noise ratio. While the microstructured dielectric enhances sensitivity, the conductive fabric electrodes ensure a secure conductive network and enable the creation of robust and flexible electrical connections through heat pressing and adhesive film technology. This is important for real-life applications where flexible, low-profile, and secure connections are required.

The inherent structural properties of conductive fabrics also cause the forming of air gaps between the dielectric and electrode layers, which act as an additional dielectric layer for increased sensitivity. It is important to understand the effect of different textile types, i.e., knitted and woven, on sensing mechanism of the proposed sensor in order to the tailor needs of end application. Thus, we also explore the effects of different conductive fabrics (knitted vs woven) on the pressure sensitivity of the soft pressure sensor and employed two different materials (sugar granules and salt crystals) to create micropores within the silicone elastomer dielectric layer to understand how pores size also affects sensor performance. We found that a combination of the conductive knit electrode and higher porosity (generated using sugar granules) yielded higher sensitivity. It should be noted here that, in previous studies, sensors manufactured via solid particle leaching methods saturated around 100 kPa as the working range is solely determined by the compressibility of the microporous dielectric layer. However, in our case, the sensor remains sensitive when pressures up to 1 MPa are applied. This level of working range is directly enabled by the integration of the knit electrode that is compressed gradually under the applied pressure due to the higher stiffness compared with microporous silicone elastomer.[49] As a practical demonstration in the realm of wearable robotics, the sensor was integrated into a glove to measure grip pressure during object manipulation.

To understand the effects of different textiles and microstructural morphologies on sensor performance, we produced four different types of the pressure sensing structures with equal dielectric layer thicknesses (960 μm). Initially, unstructured (without micropores) dielectric layers were produced, and either conductive knit or conductive woven fabrics were laminated onto the dielectric layer to form the soft capacitance-based pressure sensor. These embodiments facilitated our understanding of the effect of different textiles on the sensing properties of the pressure sensor. Thereafter, knit fabrics (which demonstrated higher sensitivity) were laminated onto the microporous dielectric layers (mpdl) created with either sugar granules or salt crystals in which we observed the effect of micropore size on sensitivity of the pressure sensor. It should be noted here that manufacturing of the capacitive sensors without mpdl followed same fabrication method, with the exception of micropore creation within the elastomer. The manufacturing process of the capacitance-based soft pressure sensor with the mpdl is shown in **Figure 1**. The process can be divided into three main steps: (1) manufacturing of the microporous silicone elastomer as a dielectric layer by integrating sugar granules or salt crystals, (2) lamination of the conductive fabrics onto the microporous dielectric layer, and (3) the creation of robust and compliant electrical connections. Figure 1a illustrates the complete manufacturing process of the structured soft pressure sensor and subsequent sensor design. Ecoflex 30 silicone elastomer and sugar granules or salt crystals were mixed in a ratio of 4:1 by weight. We chose this mixing ratio because, above this ratio, the resulting structure had a tendency to crack during separation from the 3D printed mold. Thereafter, the solution was poured into a 3D printed mold and oven-cured at 70 °C for 2 h. By immersing the cured solution in an ultrasonic washing tank for 2 h at 80 °C, the granules dissolved, leaving behind micropores within the silicone elastomers and creating an open-cell porous silicone structure.[50] After ultrasonication, conductive fabrics were laminated onto both sides of the dielectric layer using a thin film applicator with Ecoflex 30 as an adhesion layer. The sample was cured in the oven at 70 °C for 2 h, after which, individual sensors were cut from the sample using laser technology and electrical connections were attached. Using adhesive tape and a heat press to laminate conductive yarns onto the surface attained robust and compliant electrical connections. Figure 1b,c shows an actual image of the soft sensor with conductive knit electrodes as well as working mechanism of the sensor. Figure 1d,e shows the scanning electron microscopy (SEM) images of the sensor and mpdl. The amount of the porosity of the structure varied depending on the material used and the overall porosity of the mpdl found to be 44% and 30% samples produced with sugar and salt granules, respectively (Section 1,Supporting Information).

To characterize the electrical response of the sensors to applied pressure, we developed an experimental setup to collect synchronized mechanical and electrical data, using a mechanical tester (Instron 5544A, Instron, USA) and a capacitance meter (Model 3000, GLK Instruments, USA) (Figure S1, Supporting Information). A vertical load of up to the 22.5 N (corresponding to 100 kPa) was applied in a direction normal to the sensor surface. Sensors used for characterization were 15 mm × 15 mm in total area with a dielectric thickness of 960 μm and total sensor thicknesses of 1960 and 1185 μm for knit and woven electrodes, respectively.

Initially, to understand the standalone effect of conductive textile type (knitted vs woven) on the sensitivity of the proposed sensors, we tested sensors constructed from conductive textiles and an unstructured (without micropores) silicone dielectric layer. **Figure 2**a shows the electrical response of the two types of sensor under applied pressure level of 100 kPa and we calculated pressure sensitivities for each type of the sensor. The sensitivity (S) of pressure sensor can be calculated as $S = \Delta C/C_0/P$

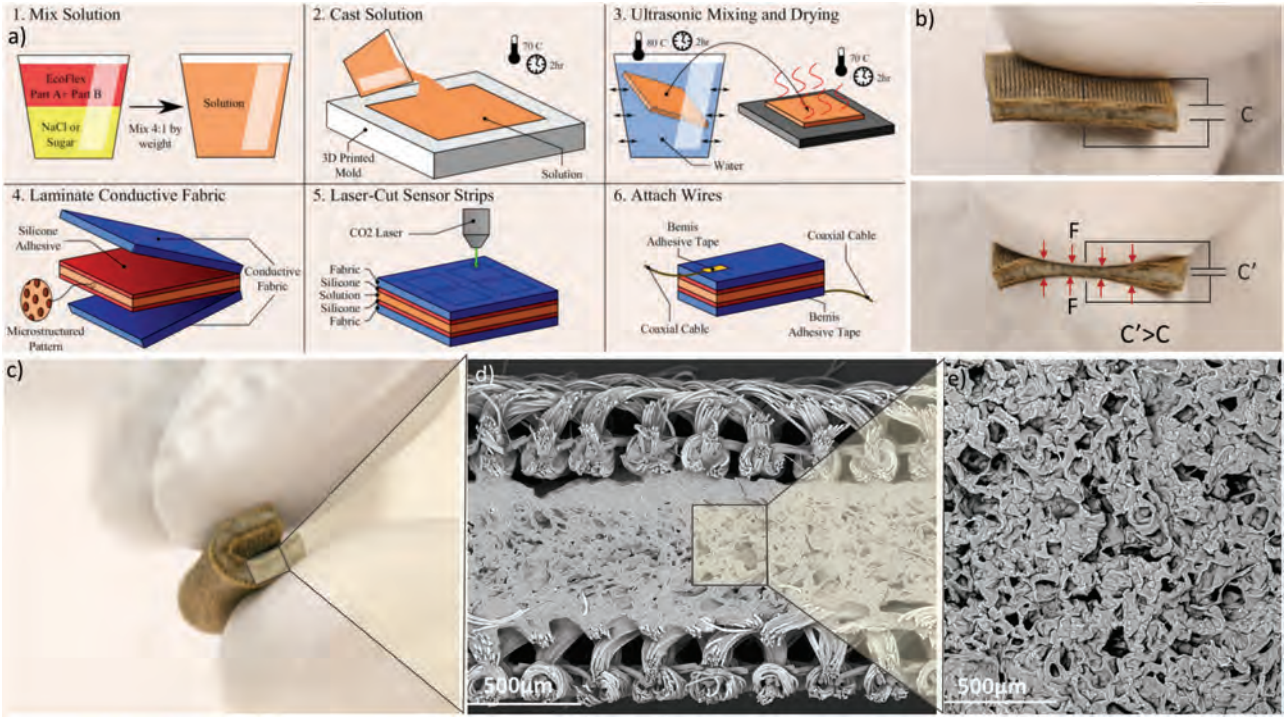

Figure 1. a) Schematic diagram of the fabrication process of the capacitive-based soft pressure sensor. b) Actual image of the sensor and general working principle under force loading. c) Actual image of the sensor in which bendability of the sensor is shown. d) Cross-sectional view of the sensor captured via SEM. e) SEM image of the mpdl.

where P represents the applied pressure, and ΔC and C_0 represent the change in capacitance and baseline capacitance, respectively. As seen in Figure 2a, while the sensor constructed with a woven electrode has a pressure sensitivity of 7×10^{-4} kPa^{-1}, the sensor with a knit electrode layer has a pressure sensitivity of 23×10^{-4} kPa^{-1}. Since the same dielectric layer and thickness was used, the difference between the pressure sensitivities stems from the inherent properties of the textile structures. In general, knitted fabrics are bulkier and their surface is not as smooth as woven fabrics. As seen in Figure 2b, there is a space between the adjacent wales of the knitted structure, and loops within these wales create connections between adjacent wales through the sinker loops which are located in back plane of the knitted structure. Thus, when the surface of the knitted fabric is laminated onto the silicone elastomer, these spaces naturally form air gaps between the silicone elastomer and the conductive surface of the fabric (Figure 2b; Figure S2, Supporting Information). These air gaps add a second dielectric layer to the sensors with knit electrodes, thereby increasing sensitivity.

On the other hand, the woven fabric (1×1 plain weave) has a relatively flat surface (as can be seen from the SEM and 3D intensity images in Figure 2b; Figure S3, Supporting Information). Thus, we observe no air gap between the electrode and the fabric layer. 3D intensity images were captured by using laser confocal microscope to quantify the height variation over the fabric surface. The deepest region of the sample is marked as zero, and the height profile of the rest of the structure is marked accordingly. Given these preliminary results, the knitted fabric electrode was chosen to construct proposed sensor with the microporous dielectric layer due to its higher sensitivity. The combination of the conductive knit fabric with the microporous dielectric layer further yielded higher sensitivity when compared with the nonporous one. As explained in earlier works in this area,[46–48] the capacitance change resulting from applied pressure is mostly based on the change in dielectric thickness for solid elastomeric dielectric layers, and as such, thickness change in the mpdl is higher compared with solid elastomer thereby yielding higher sensitivity (Figure S4, Supporting Information). Moreover, sensitivity also increases due to the gradual closure of the micropores under the applied pressure that increases the effective dielectric constant due to the displacement of air (Equations (1) and (2) below).

The capacitance of the sensor (C_{sensor}) can be described by the following parameters: electrode area (A), dielectric thickness (d), dielectric permittivity of vacuum (ε_0), and permittivity of the dielectric (ε_r). Equation (1) describes the change-in-capacitance due to variations in dielectric layer thickness

$$C_{\text{sensor}} = \varepsilon_0 \varepsilon_r \frac{A}{d_0} \tag{1}$$

In addition to the dielectric thickness change, variations in the effective relative permittivity of the dielectric (ε_e) under the pressure loading also contributes to a change in capacitance

$$\varepsilon_e = (\%V_{\text{air}} . \varepsilon_{\text{air}} + \%V_{\text{silicone}} . \varepsilon_{\text{silicone}}) \tag{2}$$

where, $\varepsilon_{\text{air}} = 1$ and $\varepsilon_{\text{silicone}} = 2.8$. Since the volume of the air gaps will reduce under the pressure loading, ε_e will increase overall, thereby increasing sensitivity.

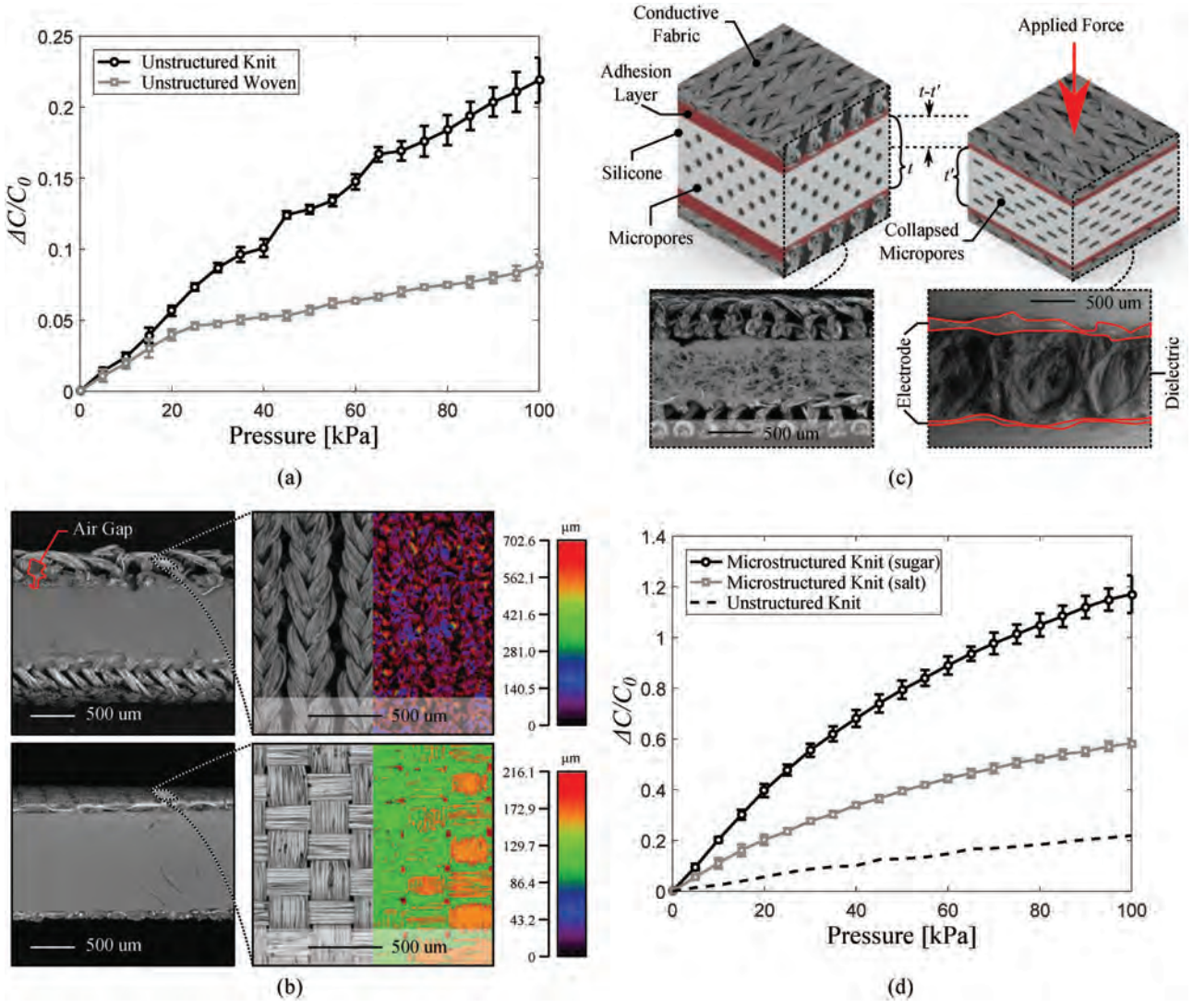

Figure 2. a) Relative change in sensors' capacitance under pressure for the sensors consists of unstructured dielectric layer with the knit and woven electrodes. b) SEM images show the surface properties of the knit and woven electrodes as well as air gaps within structure. c) Working mechanism of the microporous sensors, SEM images show before and after loading. d) Relative change in sensors' capacitance under pressure for the sensors consists of mpdl (either sugar or salt crystal) with the knit electrodes.

In our case, the use of knit conductive fabric with the mpdl further boosts the capacitance change due to the closing of the air gap between the elastomeric layer and conductive fabric, which is depicted in Figure 2c. Figure 2d shows the electrical response of the proposed sensors constructed using either sugar granules or salt crystals. Measured sensitivities were 121×10^{-4} kPa^{-1} for the sensors with sugar-generated micropores, and 45×10^{-4} kPa^{-1} for the sensors with salt-generated micropores. As the sugar granules generated higher porosity, we observe a direct correlation between the degree of the porosity and sensor performance as higher porosity leads to increased effective compliance of the dielectric layer. Moreover, we also tested the sensors up to the 1 MPa pressure level and we observed that output of the sensor signal was still below the saturation point. However, sensitivity values of the sensors reduced at this level (Figure S5, Supporting Information).

For further electromechanical characterization, we chose the sensor constructed using a combination of the conductive knit electrode and the micropores that generated using sugar granules due to its higher sensitivity. We used the same experimental set up that was used during the preliminary investigations for the characterization of the pressure sensor (described in Figure S1, Supporting Information).

The efficacy of this sensing modality as a wearable sensor is dictated by its resolution, drift, and bandwidth properties. To determine the resolution, we measured the noise in the sensor response at the maximum pressure level of 100 kPa. All measurements were obtained while maintaining a sensing bandwidth of 50 Hz. The resolution corresponds to a 95% confidence interval around the measured value. We found the absolute resolution value to be 0.86 kPa of full scale (Section 2, Supporting Information). To observe the drift under static

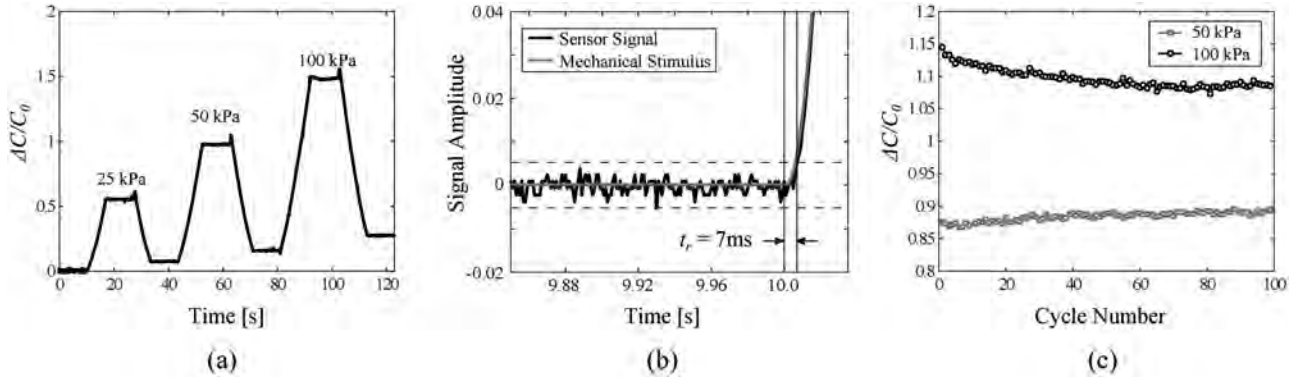

Figure 3. a) Capacitance change as a function of time for sensors subjected to step deformation at 25, 50, and 100 kPa pressure levels. b) Response time of the sensor. c) Stability of the pressure sensitivity under cyclic test.

loading, 25, 50, and 100 kPa pressure levels were applied to the capacitive sensor at a loading rate of 0.05 mm s^{-1} and held for 10 s at these pressure levels, as shown in **Figure 3**a. The drift of the capacitance values of the pressure sensor was measured to be 0.05%, 0.15%, and 0.1% for pressure levels of 25, 50, and 100 kPa, respectively, and these values can be considered negligible for the real-life applications. The response time of the sensor was calculated as the time span between mechanical stimulation and the point in time when the sensor signal rose three standard deviations above the base signal at a loading speed of 24 mm s^{-1}. The sensor's delay was found to be 7 ms (Figure 3b). Given that the frequency of body motion is usually below 10 Hz, our capacitive sensor could be considered a suitable candidate for sensing body motions. We tested the stability of the pressure sensors in terms of pressure sensitivity by performing repeated loading/unloading cyclic test (100 cycles) (Figure 3c). We found that sensitivity of the sensors changed by 2.7% and 8.4% for the pressure levels 50 and 100 kPa, respectively. We observe that, for pressure values up to the operating range of 100 kPa, the sensitivity of the sensor decreases initially but stabilizes to a steady-state value after some cyclic loading/unloading period. This could be explained as follows. The sensor we are proposing consists of a microporous dielectric layer and conductive fabric electrodes, and the deformation of both structures under applied pressure leads to a change in electrical response of the sensor. While the deformation of the microporous dielectric layer is reversible,[46] the total deformation of the textile material is equal to sum of the elastic deformation (reversible after pressure is removed) and plastic deformation (permanent) under the applied load.[8,51] However, after 40 cycles, the plastic deformation of the textile electrodes remains stable, and as such, the electrical output of the sensor becomes stable (Figure 3c). Possible future approaches to increase the stability of the proposed sensor are to increase elastic properties of the fabric electrodes by increasing elastomeric yarn (lycra) content within the fabric structure or implementation of the conditioning cycles before the practical use. We also evaluated the hysteresis of the proposed sensor up to 100 kPa pressure. Relative change-in-capacitance values were logged during the loading (increasing pressure) and unloading (decreasing pressure), and the maximum hysteresis error of the sensor was found to be 4.5% (Figure S6, Supporting Information). In previous studies,[46,47] sensors that have micropores within their structure showed negligible hysteresis and this has been attributed to the reversible closure/opening behavior of micropores within the silicone elastomer. However, the sensor we present in this paper showed slightly higher hysteresis when compared with previously reported sensors with micropores. It is possible that the fabrication methodology or the textile material properties may have contributed to this but further investigation is required.[8]

To demonstrate the potential for the sensor to be used in wearable application, the proposed sensor was integrated into a textile structure to create a smart tactile glove as can be seen in **Figure 4**a. The sensor was embedded into the thumb of the glove by applying thin layer of fabric glue (Loctite, Vinyl, Fabric & Plastic Adhesive) to distinguish objects with different weights during a grasping task. Subjects were instructed to grasp objects with thumb and index finger for a specified amount of time, and the electrical signal of the sensor was recorded. Plastic cups with different weights of water (18, 151, and 293 g) were grasped and released three times during each experiment. Figure 4b shows each capacitance change ratio ($\Delta C/C_0$) of the capacitive sensor during the three scenarios. Change in capacitance value is found to be the highest when the subject grasps the heaviest object. The result shows that the soft sensor can be utilized to sense the fingertip pressure level during the grasp action and we anticipate that this kind of the soft sensor can be used where the robotic control is needed.

In summary, a highly sensitive soft pressure sensor based on conductive fabrics and mpdl is proposed. Initially, different types of conductive fabrics (knitted and woven) were evaluated as electrodes and were laminated onto a nonporous dielectric layer in order to observe effect of fabric structure on the sensitivity of the proposed sensor. Thereafter, knitted fabrics (which were observed to have higher sensitivity) were combined with mpdl in order to create a highly sensitive pressure sensor. Mpdl is prepared using a solid particle leaching method using sugar granules and salt crystals. The combination of the conductive knit electrode and higher porosity (generated using sugar granules) yielded the highest sensitivity (121×10^{-4} kPa^{-1}). Use of conductive knit electrode can also be combined with other approaches to build flexible capacitive sensors with a variety of attributes and performance specifications. Finally, we demonstrated the application of

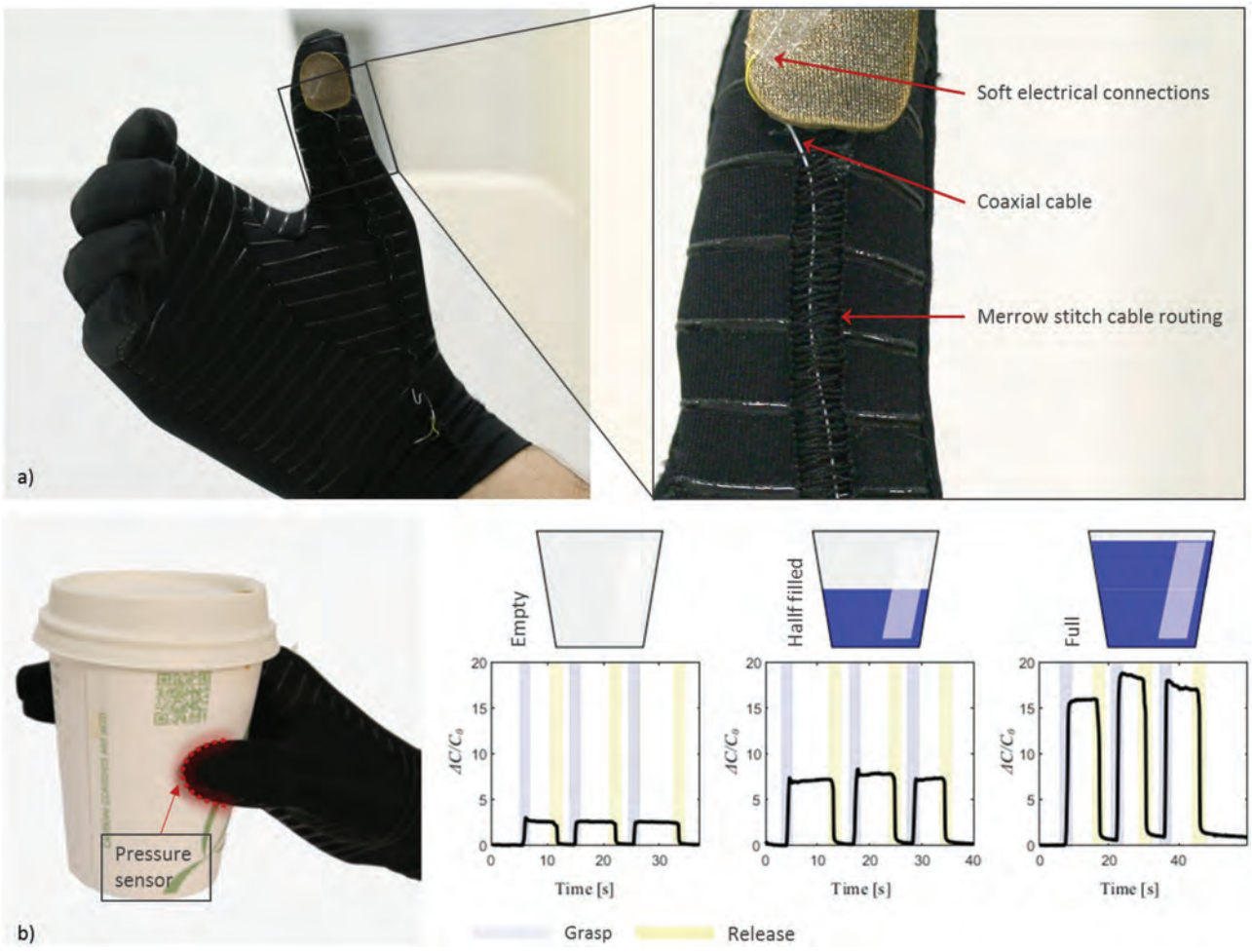

Figure 4. a) An image shows the sensing glove with its components. b) Graphics shows the change in capacitance values when the subject grasps the different amount weights.

the soft pressure sensor for the detection of grasping force via the integration of the sensor into the textile glove. Such sensors could also be used in soft wearable robotics application for control purposes.

Experimental Section

Manufacturing of Nonstructured Dielectric Layer: To fabricate the silicone elastomer, Ecoflex 30 (from Smooth-On) Parts A and B were mixed in a ratio of 1:1 by weight with a centrifugal planetary mixer (ARE-310, Thinky Mixer, USA) for 60 s. Thereafter, the liquid silicone mixture (2.5 g) was subsequently poured into the 3D printed molds. The mixture was degassed at −30 psi for 3 min before curing in the oven at 70 °C for 2 h.

Manufacturing of Microporous Dielectric Layer: To fabricate the microporous silicone dielectric layer, silicone elastomer was prepared as described in the section of manufacturing of nonstructured dielectric layer. Thereafter, prepared silicone solution was mixed with solid particles (either salt granules or salt crystal) in a ratio of 4:1 by weight. Thereafter, the solution was poured into 3D printed molds and oven-cured at 70 °C for 2 h. By immersing the cured solution in an ultrasonic washing tank for 2 h at 80 °C, the granules dissolved, leaving behind micropores within the silicone elastomers.

Lamination of the Conductive Textiles onto Dielectric Layer to Create Sensor Mat: lamination layer was cast from prepared silicone material using an automatic film applicator (4340, Elcometer Inc., USA) set to speed 0 with an adjustable Baker film applicator (3530/3, Elcometer Inc.) set to a height of 200 µm. Thereafter, conductive textile was placed on to this layer and pressed with a roller to ensure secure adhesion. This process was repeated for other electrode as well. Whole system was cured at 70 °C for 2 h.

Cutting of Individual Sensors and Electrical Connections: Sensors were cut to designed size from the prepared mat, i.e., 15 mm × 15 mm by a laser (VLS 6.60, Universal Laser Systems, USA) at 100 W power and 50% speed setting. Microcoaxial cable (50MCX-37, Molex Temp-Flex) was used for electrical connections. Core and sheath wires were attached using thermal seam tape with iron at 150 °C pressed for 10 s.

Surface Characterization of Conductive Fabrics: Surface characteristics of the conductive fabrics were obtained using SEM for high-resolution images and laser scanning digital microscope (Olympus LEXT OLS4100) for the height information of the samples.

Electromechanical Characterization of Capacitive Sensors: Sensors were dynamically tested in the tensile testing machine, and capacitance was measured during testing with a capacitance meter (Model 3000, GLK instruments CA, USA). Load, extension, and capacitance data were synchronously logged via a common I/O interface, (bNC-2111, national Instruments Corp.).

Supporting Information

Supporting Information is available from the Wiley Online Library or from the author.

Acknowledgements

This material was based upon the work supported by the National Science Foundation (Grant No. CBET-1454472), the Scientific and the Defense Advanced Research Projects Agency (DARPA), the Warrior Web Program (Contract No. W911NF-14-C-0051), the Wyss Institute, and the John A. Paulson School of Engineering and Applied Sciences at Harvard University. The authors also would like to thank James Weaver for SEM images.

Conflict of Interest

The authors declare no conflict of interest.

Keywords

capacitive sensors, conductive fabrics, microporous dielectric layers, soft pressure sensors

Received: September 1, 2017
Revised: October 6, 2017
Published online:

[1] T. Q. Trung, N.-E. Lee, *Adv. Mater.* **2016**, *28*, 4338.
[2] G. Schwartz, B. C. Tee, J. Mei, A. L. Appleton, D. H. Kim, H. Wang, Z. Bao, *Nat. Commun.* **2013**, *4*, 1859.
[3] J. Lee, H. Kwon, J. Seo, S. Shin, J. H. Koo, C. Pang, S. Son, J. H. Kim, Y. H. Jang, D. E. Kim, *Adv. Mater.* **2015**, *27*, 2433.
[4] M. Weigel, A. S. Nittala, A. Olwal, J. Steimle, presented at *Proc. of the 2017 CHI Conf. on Human Factors in Computing Systems*, Denver, May, **2017**.
[5] W. Zeng, L. Shu, Q. Li, S. Chen, F. Wang, X. M. Tao, *Adv. Mater.* **2014**, *26*, 5310.
[6] C. A. Cezar, E. T. Roche, H. H. Vandenburgh, G. N. Duda, C. J. Walsh, D. J. Mooney, *Proc. Natl. Acad. Sci. USA* **2016**, *113*, 1534.
[7] Y. Mengüç, Y.-L. Park, H. Pei, D. Vogt, P. M. Aubin, E. Winchell, L. Fluke, L. Stirling, R. J. Wood, C. J. Walsh, *Int. J. Rob. Res.* **2014**, *33*, 1748.
[8] A. Atalay, V. Sanchez, O. Atalay, D. M. Vogt, F. Haufe, R. J. Wood, C. J. Walsh, *Adv. Mater. Technol.* **2017**, *2*, 1700136.
[9] O. Atalay, A. Atalay, J. Gafford, H. Wang, R. Wood, C. Walsh, *Adv. Mater. Technol.* **2017**, *2*, 1700081.
[10] N. Lu, D.-H. Kim, *Soft Rob.* **2014**, *1*, 53.
[11] D. Rus, M. T. Tolley, *Nature* **2015**, *521*, 467.
[12] Y. Gao, H. Ota, E. W. Schaler, K. Chen, A. Zhao, W. Gao, H. M. Fahad, Y. Leng, A. Zheng, F. Xiong, C. Zhang, L.-C. Tai, P. Zhao, R. S. Fearing, A. Javey, *Adv. Mater.* **2017**, *29*, 1701985.
[13] L. N. Awad, J. Bae, K. O'Donnell, S. M. De Rossi, K. Hendron, L. H. Sloot, P. Kudzia, S. Allen, K. G. Holt, T. D. Ellis, *Sci. Transl. Med.* **2017**, *9*, eaai9084.
[14] B. Quinlivan, S. Lee, P. Malcolm, D. Rossi, M. Grimmer, C. Siviy, N. Karavas, D. Wagner, A. Asbeck, I. Galiana, *Sci. Rob.* **2017**, *2*, eaah4416.
[15] P. Polygerinos, Z. Wang, K. C. Galloway, R. J. Wood, C. J. Walsh, *Rob. Auton. Syst.* **2015**, *73*, 135.
[16] D. P. Holland, E. J. Park, P. Polygerinos, G. J. Bennett, C. J. Walsh, *Soft Rob.* **2014**, *1*, 224.
[17] S. Jung, J. H. Kim, J. Kim, S. Choi, J. Lee, I. Park, T. Hyeon, D. H. Kim, *Adv. Mater.* **2014**, *26*, 4825.
[18] S. M. M. De Rossi, N. Vitiello, T. Lenzi, R. Ronsse, B. Koopman, A. Persichetti, F. Vecchi, A. J. Ijspeert, H. Van der Kooij, M. C. Carrozza, *Sensors* **2010**, *11*, 207.
[19] a) A. Ahmed, S. L. Zhang, I. Hassan, Z. Saadatnia, Y. Zi, J. Zu, Z. L. Wang, *Extreme Mech. Lett.* **2017**, *13*, 25; b) C. L. Choong, M. B. Shim, B. S. Lee, S. Jeon, D. S. Ko, T. H. Kang, J. Bae, S. H. Lee, K. E. Byun, J. Im, *Adv. Mater.* **2014**, *26*, 3451.
[20] B. C. K. Tee, A. Chortos, R. R. Dunn, G. Schwartz, E. Eason, Z. Bao, *Adv. Funct. Mater.* **2014**, *24*, 5427.
[21] Y. Zang, F. Zhang, C.-A. Di, D. Zhu, *Mater. Horiz.* **2015**, *2*, 140.
[22] A. P. Gerratt, H. O. Michaud, S. P. Lacour, *Adv. Funct. Mater.* **2015**, *25*, 2287.
[23] S. Gong, W. Schwalb, Y. Wang, Y. Chen, Y. Tang, J. Si, B. Shirinzadeh, W. Cheng, *Nat. Commun.* **2014**, *5*, 3132.
[24] M. Weigel, T. Lu, G. Bailly, A. Oulasvirta, C. Majidi, J. Steimle, presented at *Proc. 33rd Annual ACM Conf. on Human Factors in Computing Systems*, Seoul, April, **2015**.
[25] L. Viry, A. Levi, M. Totaro, A. Mondini, V. Mattoli, B. Mazzolai, L. Beccai, *Adv. Mater.* **2014**, *26*, 2659.
[26] S. D. Min, Y. Yun, H. Shin, *IEEE Sens. J.* **2014**, *14*, 3245.
[27] M. G. Mohammed, R. Kramer, *Adv. Mater.* **2017**, *29*, 1604965.
[28] L. Qiu, M. Bulut Coskun, Y. Tang, J. Z. Liu, T. Alan, J. Ding, V. T. Truong, D. Li, *Adv. Mater.* **2016**, *28*, 194.
[29] L.-Q. Tao, K.-N. Zhang, H. Tian, Y. Liu, D.-Y. Wang, Y.-Q. Chen, Y. Yang, T.-L. Ren, *ACS Nano* **2017**, *11*, 8790.
[30] Y.-L. Park, C. Majidi, R. Kramer, P. Bérard, R. J. Wood, *J. Micromech. Microeng.* **2010**, *20*, 125029.
[31] O. A. Araromi, C. J. Walsh, R. J. Wood, presented at *Sensors, 2016 IEEE*, Orlando, November, **2016**.
[32] C. Dagdeviren, P. Joe, O. L. Tuzman, K.-I. Park, K. J. Lee, Y. Shi, Y. Huang, J. A. Rogers, *Extreme Mech. Lett.* **2016**, *9*, 269.
[33] C. Dagdeviren, Y. Shi, P. Joe, R. Ghaffari, G. Balooch, K. Usgaonkar, O. Gur, P. L. Tran, J. R. Crosby, M. Meyer, *Nat. Mater.* **2015**, *14*, 728.
[34] M. Amjadi, K. U. Kyung, I. Park, M. Sitti, *Adv. Funct. Mater.* **2016**, *26*, 1678.
[35] A. Chortos, Z. Bao, *Mater. Today* **2014**, *17*, 321.
[36] S. C. Mannsfeld, B. C. Tee, R. M. Stoltenberg, C. V. H. Chen, S. Barman, B. V. Muir, A. N. Sokolov, C. Reese, Z. Bao, *Nat. Mater.* **2010**, *9*, 859.
[37] A. P. Robinson, I. Minev, I. M. Graz, S. P. Lacour, *Langmuir* **2011**, *27*, 4279.
[38] Y. Shu, H. Tian, Y. Yang, C. Li, Y. Cui, W. Mi, Y. Li, Z. Wang, N. Deng, B. Peng, *Nanoscale* **2015**, *7*, 8636.
[39] B. Zhu, Z. Niu, H. Wang, W. R. Leow, H. Wang, Y. Li, L. Zheng, J. Wei, F. Huo, X. Chen, *Small* **2014**, *10*, 3625.
[40] S. Lee, A. Reuveny, J. Reeder, S. Lee, H. Jin, Q. Liu, T. Yokota, T. Sekitani, T. Isoyama, Y. Abe, *Nat. Nanotechnol.* **2016**, *11*, 472.
[41] K. F. Lei, K.-F. Lee, M.-Y. Lee, *Microsyst. Technol.* **2014**, *20*, 1351.
[42] B.-Y. Lee, J. Kim, H. Kim, C. Kim, S.-D. Lee, *Sens. Actuators, A* **2016**, *240*, 103.
[43] H. Zhang, M. Y. Wang, J. Li, J. Zhu, *Smart Mater. Struct.* **2016**, *25*, 035045.
[44] Y. Song, H. Chen, Z. Su, X. Chen, L. Miao, J. Zhang, X. Cheng, H. Zhang, *Small* **2017**, *13*, 1702091.
[45] J.-W. Han, B. Kim, J. Li, M. Meyyappan, *Appl. Phys. Lett.* **2013**, *102*, 051903.
[46] D. Kwon, T.-I. Lee, J. Shim, S. Ryu, M. S. Kim, S. Kim, T.-S. Kim, I. Park, *ACS Appl. Mater. Interfaces* **2016**, *8*, 16922.

[47] D. Kwon, T.-I. Lee, M. Kim, S. Kim, T.-S. Kim, I. Park, presented at *2015 Transducers - 2015 18th Int. Conf. on Solid-State Sensors, Actuators and Microsystems (TRANSDUCERS)*, Alaska, June, **2015**.
[48] J. I. Yoon, K. S. Choi, S. P. Chang, *Microelectron. Eng.* **2017**, *179*, 60.
[49] P. Polygerinos, B. Mosadegh, A. Campo, PneuNets Bending Actuators, https://softroboticstoolkit.com/book/pneunets-variation-material (accessed: September, 2017).
[50] W. Yang, Y. G. Nam, B.-K. Lee, K. Han, T. H. Kwon, D. S. Kim, *Jpn. J. Appl. Phys.* **2010**, *49*, 06GM01.
[51] L. Guo, L. Berglin, H. Mattila, *Text. Res. J.* **2012**, *82*, 1937.